A Multi-agent Framework for Materials Laws Discovery

Bo Hu[3], Siyu Liu[1,2], Beilin Ye[1], Yun Hao[4], and Tongqi Wen[1,2*]

[1]*Center for Structural Materials, Department of Mechanical Engineering, The University of Hong Kong, Hong Kong, China*
[2]*Materials Innovation Institute for Life Sciences and Energy (MILES), The University of Hong Kong, Shenzhen, China*
[3]*Weiyang College, Tsinghua University, Beijing, China and*
[4]*School of Software Engineering, South China University of Technology, Guangzhou, China*
(Dated: November 26, 2024)

Uncovering the underlying laws governing correlations between different materials properties, and the structure-composition-property relationship, is essential for advancing materials theory and enabling efficient materials design. With recent advances in artificial intelligence (AI), particularly in large language models (LLMs), symbolic regression has emerged as a powerful method for deriving explicit formulas for materials laws. LLMs, with their pre-trained, cross-disciplinary knowledge, present a promising direction in "AI for Materials". In this work, we introduce a multi-agent framework based on LLMs specifically designed for symbolic regression in materials science. We demonstrate the effectiveness of the framework using the glass-forming ability (GFA) of metallic glasses as a case study, employing three characteristic temperatures as independent variables. Our framework derived an interpretable formula to describe GFA, achieving a correlation coefficient of up to 0.948 with low formula complexity. This approach outperforms standard packages such as GPlearn and demonstrates a ∼30% improvement over random generation methods, owing to integrated memory and reflection mechanisms. The proposed framework can be extended to discover laws in various materials applications, supporting new materials design and enhancing the interpretation of experimental and simulation data.

Discovering fundamental physical laws is essential for understanding experimental phenomenon and solving theoretical challenges. These laws can be derived theoretically or discovered from experimental data. For example, Kepler's laws exemplify how physical laws can be uncovered through data analysis [1]. In material science, vast amounts of data are generated annually from experiments and simulations. Since the launch of the Materials Genome Initiative [2], many databases were established, such as Materials Project [3], AFLOW [4, 5], ICSD [6] and Materials Cloud [7]. These databases have substantially advanced our understanding of structure-property relationships and enhanced the efficiency of materials design. To further improve our knowledge in materials design, it is crucial to identify governing material laws between structure/composition and materials properties [8], such as mechanical, electrical and thermal properties. Uncovering these relationships will deepen our understanding of material behaviors and improve our ability to design materials with specific properties.

Various artificial intelligence (AI) methods, such as machine learning and deep learning, are widely applied in analyzing materials property data [9, 10] and generating predictive models. Although these models sometimes yield accurate property predictions, they typically function as "black boxes", where relationships between structure and property remain obscured. This lack of interpretability limits insights into fundamental materials laws. Symbolic regression (SR) [11, 12] offers a solution to this problem by identifying explicit mathematical formulas that describe datasets, thus uncovering structure-property relationships more transparently. Traditionally, SR tasks have been approached using Genetic Programming (GP) [13] algorithm, which structures formulas as trees and uses genetic operations like mutation and crossover to interactively optimize formulas. With advancements in AI, more SR algorithms emerged, including deep learning-based SR [14, 15], Transformer-based SR [16] and graph SR [17]. These approaches have been successfully employed in materials science to identify key descriptors of materials properties [18], guide the design of new materials and reveal quantitative structure-property relationships.

In recent years, large language models (LLMs) have demonstrated impressive capabilities in various fields, especially in generating complex content across scientific and mathematical contexts. Built on Transformer structures and pre-trained on vast knowledge bases, LLMs have become a promising foundation for developing new SR algorithms aimed at deriving mathematical or scientific equations [19–21]. This extensive pre-training allows LLMs to leverage exisiting scientific knowledge, narrowing the search space in symbolic regression by starting from established concepts rather than random initialization. LLM-based SR approaches have shown success in deriving equations from datasets rooted in known scientific principles, such as formulas from Feynman's lectures [1], achieving near perfect correlation (R^2 close to 0.99) with ground truth values. However, in material science, data is often from experiments, presenting challenges such as sparsity and inherent measurement errors. These factors complicate the discovery of materials laws and quantitative relationships, making the use of LLMs for deriving accurate structure-property formulas in materials science a complex but promising approach.

In this paper, we present a general multi-agent framework [22, 23] leveraging LLMs to address symbolic regression challenges in discovering physical laws for materials science. Our approach incorporates the depth-first search (DFS) algorithm and a reflection mechanism [24, 25], implemented through LLMs, to optimize the formula generation process. The framework operates as follows: (i) define the problem and prepare the dataset; (ii) design effective prompts with clear

* tongqwen@hku.hk

task descriptions, datasets, operators and evaluation criteria; (iii) set hyperparameters for DFS to initiate the optimization; (iv) retrieve results and assess the generated formulas; (v) apply accurate formulas to downstream tasks. We demonstrate this framework by tackling the problem of predicting the glass-forming ability (GFA) in metallic glasses (MGs) [26–28], using characteristic temperatures and GFA data from 23 types of MGs to derive predictive formulas. An additional test set of 33 MGs is used to evaluate the performance of these formulas. Our results indicate that the derived formulas achieve high accuracy, with a maximum correlation ($R^2 = 0.948$) with the critical cooling rate R_c for the test set, while maintaining low formula complexity. This approach shows better performance compared to reported formulas and conventional GP algorithms, requires less human intervention and narrows the search space. The DFS trajectory memory enhances formula accuracy by ∼30% over random guessing by LLMs and the reflection mechanism further optimizes formula complexity and accuracy. The generated formula with low complexity can be easily interpreted based on domain knowledge. This LLM-based multi-agent framework is extendable to other materials science problems, promoting the advancement of materials theories and laws.

Multi-agent Framework for Symbolic Regression

FIG. 1 shows the schematic workflow of our multi-agent framework. The framework operates through DFS, where each DFS iteration includes loops managed by multiple agents (FIG. 1(a)). The formulas generation workflow consists of several DFS iterations and output the final formulas (FIG. 1(b)).

In the detailed workflow FIG. 1, formula generation begins with a customized prompt to guide the LLMs. This prompt has 4 sections: "General Instruction", "Task Description", "Formula Memory" and "Output Requirements" (see Supplementary Fig. S1). The "General Instruction" provides the LLMs with essential information about the formula generation process and tips to minimize hallucinations. Then "Task Description" outlines the specific problem, including background, dataset and operators details, evaluation criteria, and requirements like unit consistency. "Formula Memory" contains low-scoring formulas with good performance and feedback from the "Self-reflection" agent to prevent redundant solutions and enable the LLM to refine outputs based on prior attempts [29]. Finally, "Output requirements" constrains the response format by providing an example; the LLM is instructed to output in a strict format, such as "F = %Function%", where "%Functions%" is replaced by the generated formula expression, with no extraneous descriptive text allowed.

Using this prompt, the LLM generates candidate formulas, which are then translated into executable code for evaluation in Python. Each formula undergoes a preliminary inspection to identify and prevent potential calculation errors. For example, certain data points might lead to divisions by zero within a formula, thus interrupting the calculation process. To address this, we evaluate each generated formula with the dataset to check for such issues. If any formula produces errors with specific data points, it is automatically excluded from further analysis.

In the evaluation phase, we apply the criteria from [16], which assesses both accuracy and complexity of the generated formulas:

$$r\left(\hat{f}(\mathbf{x})|y\right) = \frac{1}{1 + \text{NMSE}(\hat{f}(\mathbf{x}), y)} + \lambda \exp\left(-\frac{\mathcal{C}(\hat{f})}{L}\right) \quad (1)$$

where y is the ground truth, $\hat{f}(\mathbf{x})$ is the predicted result, and NMSE is the Normalized Mean Square Error, defined as:

$$\text{NMSE}(\hat{f}(\mathbf{x}), y) = \frac{\sum_{i=1}^{N}(y_i - \hat{f}(\mathbf{x}_i))^2}{\sum_{i=1}^{N} y_i^2 + \epsilon} \quad (2)$$

where ϵ is a small constant to prevent division by zero. The first term in Eq. (1) captures the accuracy of the regression, while the second term addresses formula complexity. L is the maximum sequence length [19] (set to 30 in this work), and λ is a hyperparameter that adjusts the weighting between accuracy and complexity (evaluated in Supplementary Fig. S4). The complexity $\mathcal{C}(\hat{f})$ is defined as the number of operators in the formula. For clarity in analysis, we define the score $s(\hat{f}(\mathbf{x})|y) = r(\hat{f}(\mathbf{x})|y)^{-1}$, where a lower score indicates better performance. To optimize search efficiency, we instruct the LLM to exclude specific constants from the formula during generation and instead use variables like $a, b, c, ...$ In the evaluation step, these constants are then optimized to minimize the score, with the minimized score being taken as the final performance metric of the formula.

We adopt DFS to optimize formula generation, enhanced by a memory mechanism that record DFS trajectories for more informed feedback to the LLMs. Once scores for new formulas are calculated, each formula and its corresponding score are stored sequentially as a search trajectory, formatted as "(F0 = ...: Score0) − > (F1 = ...: Score1) − > ...", as shown in Fig. 1(a). Incorporating a self-reflection step further refines this process by having an additional LLM agent review the search trajectory from previous steps [24], offering insights to guide the next generation of formulas. This agent evaluates and provides suggestions based on the current trajectory, helping the LLM learn from past outputs. Additionally, the self-reflection agent checks for any formulas that violate preset requirements (e.g., units and operator constraints) due to model hallucinations. This ensures that the next iteration avoids generating invalid formulas, preserving a meaningful search space.

To enhance exploration and reduce dependence on initial formulas, DFS promotes diversity in generated formulas while providing a clear map of the formula evolution process. DFS is governed by two hyperparameters: maximum search depth D and the number of formulas N generated per loop. At each depth level ($d = 1, 2, ..., D$), up to N^d new formulas may be generated, where each child node in Fig. 1(b) includes the search trajectory from its parent node for deeper exploration. When the maximum depth D is reached, the search
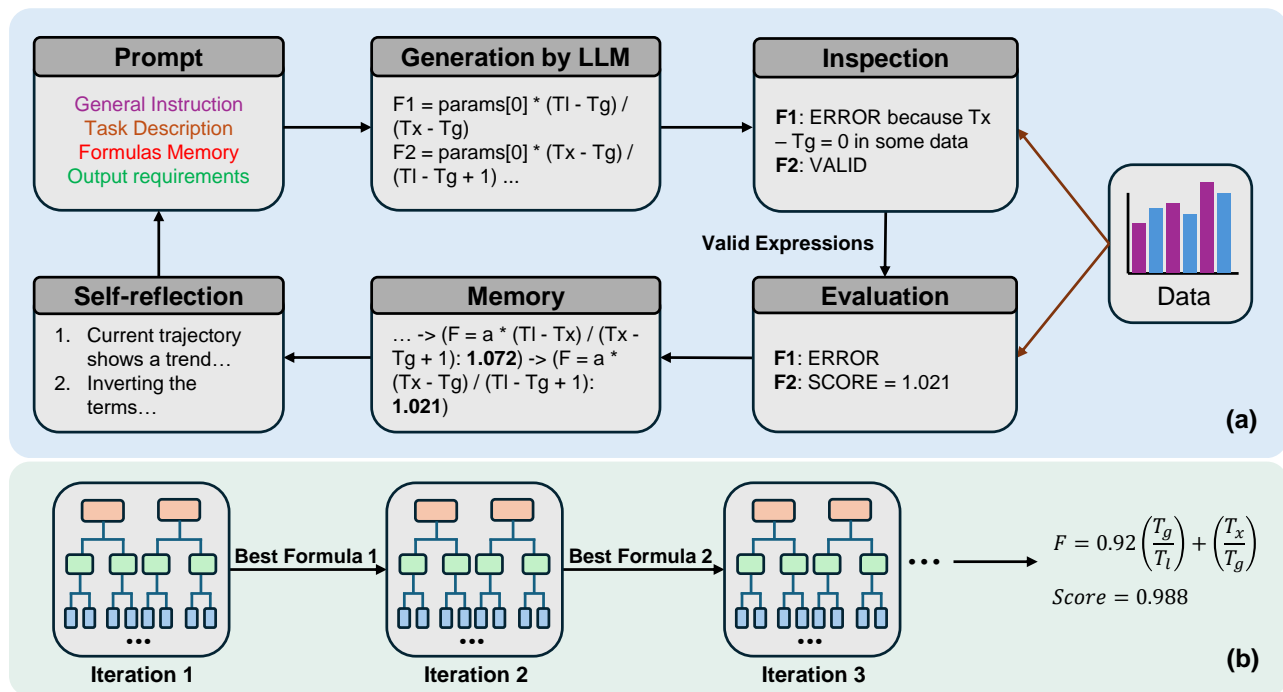
FIG. 1. Schematic workflow of the multi-agent framework. (a) Overview of the depth-first search (DFS) algorithms with the support of multiple agents. (b) Final formulas and scores are obtained after multiple DFS iterations, with each DFS iteration reaching a maximum search depth of 4 in this study.

backtracks to explore alternative paths until the optimal formula is identified or all paths are exhausted. Given the inherent randomness in the text generation by LLMs [30], we run repeated DFS processes to achieve stable, optimized result. As shown in FIG. 1(b), the best formulas from each iteration are stored as "long-term memory" and are used in subsequent iterations. This iterative approach yields the final optimized formulas once all search paths are completed.

Application: Glass-forming Ability of Metallic Glasses

To demonstrate the capabilities of our multi-agent SR framework, we apply it to investigate the glass-forming ability (GFA) of MGs. GFA describes the propensity of an alloy to form an amorphous structure under specific conditions [31]. The critical cooling rate R_c is commonly used as an accurate measure of GFA, where a lower R_c indicates a higher GFA. However, determining R_c experimentally is often labor-intensive and costly, complicating precise GFA evaluation [32]. Fortunately, certain parameters that are functions of characteristic temperatures – including the glass transition temperature T_g, onset crystallization temperature T_x and liquidus temperature T_l – can serve as effective, quantitative criteria for GFA [33]. To assess the predictive power of these parameters, we calculated the square of the correlation coefficient (R^2) between these parameters and logarithm of the critical cooling rate R_c. This approach allows us to measure how well each parameter correlates with GFA. Several previously established parameters, such as $\Delta T_x = T_x - T_g$ [34]

and $T_{rg} = T_g/T_l$ [26], are listed in Table I for reference. Two common features are observed across the parameters in Table I: most parameters are dimensionless (T_g, T_x and T_l are all in Kelvin), and they use 5 types of operators $[+, -, \times, /, \hat{}]$. To enable direct comparison between our results and these reported parameters, we generated new GFA indicators using our framework while adhering to these features.

For this specific task, we design the task description section in the initial prompt that provides a brief background on GFA, defines key quantities, such as T_g, T_x, T_l, along with the operators set $[+, -, \times, /, \hat{}]$ and evaluation criteria. For training, we use 23 MGs to derive formulas, while a separate set of 33 MGs as the test set to evaluate model performance. We selected the top formula ($F = 0.76(T_g/T_l) - T_g/T_x$) on the training set from experiments and evaluated its corresponding R^2 value on the test set, as shown in Fig. 2(a). The generated formula demonstrates a strong correlation with $\log R_c$, achieving an $R^2 > 0.94$ on the test set (not included in the training process).

Fig. 3(a) shows the kernel density plot of $\log R_c$ for both the training and test sets, indicating that the training data has a narrower distribution range for $\log R_c$ compared to the test data. Specifically, the training set values for R_c range from 0.1 to 9.15×10^5 K/s ($-2.3 \leq \log R_c \leq 13.7$), while the test set has R_c values spanning from 0.067 K/s to R_c is 3×10^{10} K/s ($-2.7 \leq \log R_c \leq 24.1$). Notably, $\sim 24\%$ of the test data fall outside the range of the training data, classifying them as "out-of-domain" data. Despite this, the generated formula performs well even for these "out-of-domain" cases, demonstrating both robust interpolation and extrapolation ability of

TABLE I. Parameters used to characterize glass-forming ability (GFA), along with their respective accuracy (R^2) and formula complexity (measured by the number of operators).

No.	Parameters	Formulas	R^2 on test data	Complexity	Ref
1	T_{rg}	$T_{\mathrm{rg}} = T_{\mathrm{g}}/T_{\mathrm{l}}$	0.826	1	[26]
2	ΔT_{x}	$\Delta T_{\mathrm{x}} = T_{\mathrm{x}} - T_{\mathrm{g}}$	0.798	1	[34]
3	γ	$\gamma = T_{\mathrm{x}}/(T_{\mathrm{g}} + T_{\mathrm{l}})$	0.932	2	[32]
4	ΔT_{rg}	$\Delta T_{\mathrm{rg}} = (T_{\mathrm{x}} - T_{\mathrm{g}})/(T_{\mathrm{l}} - T_{\mathrm{g}})$	0.730	3	[35]
5	α	$\alpha = T_{\mathrm{x}}/T_{\mathrm{l}}$	0.907	1	[36]
6	β	$\beta = T_{\mathrm{x}}/T_{\mathrm{g}} + T_{\mathrm{g}}/T_{\mathrm{l}}$	0.941	3	[36]
7	δ	$\delta = T_{\mathrm{x}}/(T_{\mathrm{l}} - T_{\mathrm{g}})$	0.772	2	[37]
8	γ_m	$\gamma_m = (2T_{\mathrm{x}} - T_{\mathrm{g}})/T_{\mathrm{l}}$	0.928	3	[38]
9	φ	$\varphi = T_{\mathrm{g}}/T_{\mathrm{l}}((T_{\mathrm{x}} - T_{\mathrm{g}})/T_{\mathrm{g}})^{0.143}$	0.891	5	[39]
10	ξ	$\xi = T_{\mathrm{g}}/T_{\mathrm{l}} + (T_{\mathrm{x}} - T_{\mathrm{g}})/T_{\mathrm{x}}$	0.937	4	[40]
11	β	$\beta = T_{\mathrm{x}}T_{\mathrm{g}}/(T_{\mathrm{l}} - T_{\mathrm{x}})^2$	0.496	4	[41]
12	ω	$\omega = T_{\mathrm{g}}/T_{\mathrm{x}} - 2T_{\mathrm{g}}/(T_{\mathrm{g}} + T_{\mathrm{l}})$	0.945	5	[42]
13	ω	$\omega = T_{\mathrm{l}}(T_{\mathrm{l}} + T_{\mathrm{x}})/(T_{\mathrm{l}} - T_{\mathrm{x}})T_{\mathrm{x}}$	0.475	5	[43]
14	θ	$\theta = (T_{\mathrm{g}} + T_{\mathrm{x}})/T_{\mathrm{l}} \cdot [(T_{\mathrm{x}} - T_{\mathrm{g}})/T_{\mathrm{l}}]^{0.0728}$	0.881	6	[44]
15	γ_c	$\gamma_c = (3T_{\mathrm{x}} - 2T_{\mathrm{g}})/T_{\mathrm{l}}$	0.929	4	[45]
16	G_p	$G_p = T_{\mathrm{g}}(T_{\mathrm{x}} - T_{\mathrm{g}})/(T_{\mathrm{l}} - T_{\mathrm{x}})^2$	0.454	5	[46]
17	χ'	$\chi' = (T_{\mathrm{x}} - T_{\mathrm{g}})/(T_{\mathrm{l}} - T_{\mathrm{x}})[T_{\mathrm{x}}/(T_{\mathrm{l}} - T_{\mathrm{x}})]^{1.47}$	0.381	7	[47]
18	γ_n	$\gamma_n = (5T_{\mathrm{x}} - 3T_{\mathrm{g}})/T_{\mathrm{l}}$	0.930	4	[48]
19	ν	$\nu = T_{\mathrm{x}}T_{\mathrm{g}}(T_{\mathrm{x}} - T_{\mathrm{g}})/(T_{\mathrm{l}} - T_{\mathrm{x}})^3$	0.328	6	[28]
20	k	$k = T_{\mathrm{x}}T_{\mathrm{g}}T_{\mathrm{l}}(T_{\mathrm{x}} - T_{\mathrm{g}})/(T_{\mathrm{l}} - T_{\mathrm{x}})^4$	0.271	7	[49]
21	G-FAS	$\text{G-FAS} = T_{\mathrm{x}}/T_{\mathrm{l}} + (T_{\mathrm{x}} - T_{\mathrm{g}})/(T_{\mathrm{l}} - T_{\mathrm{g}})$	0.888	5	[27]
22	G-FAS$_{\mathrm{m}}$	$\text{G-FAS}_{\mathrm{m}} = T_{\mathrm{x}}/T_{\mathrm{l}} + (T_{\mathrm{x}} - T_{\mathrm{g}})/(1.5T_{\mathrm{x}} - T_{\mathrm{g}})$	0.951	6	[27]

the derived formula from our framework.

To assess the effectiveness of our method, we compare its performance with that of the genetic programming (GP) algorithm and previously reported parameters in Table I. GPlearn is a widely used Python package that extends the scikit-learn machine learning library to solve symbolic regression tasks [50]. Several hyperparameters control the evolution process in GP. To obtain the best-performing formulas, we performed a grid search over these hyperparameters [18], using normalized mean squared error (NMSE) as the evaluation metric. The specific hyperparameter configurations are provided in Supplementary Table S3. From the generations produced by GPlearn, we selected the top three formulas, and their performance on the test set is presented in Fig. 2(b). The best R^2 value obtained from GPlearn is 0.943, which is slightly lower than the performance of our framework. Furthermore, for the "out-of-domain" data, which have $\log R_c$ greater than 20, the deviations of the data points from the regression line are more pronounced in the GPlearn results compared to our method, indicating weaker extrapolation ability for GPlearn.

We also evaluated the performance of other reported parameters used to characterize GFA on the test dataset. To enable a fair comparison with all baseline methods, we set two evaluation criteria: accuracy (measured by R^2) and com-plexity (number of operators in the formula). The results from our framework, along with other baseline methods, are shown in Fig. 3(b). While formula complexity can influence accuracy, higher complexity may reduce the interpretability of the model. The best formula generated by our method, $F = 0.76(T_{\mathrm{g}}/T_{\mathrm{l}}) - T_{\mathrm{g}}/T_{\mathrm{x}}$, achieves an $R^2 = 0.948$ with relatively low complexity (4 operators). In contrast, the formula with the best $R^2 = 0.943$ from GPlearn has a much higher complexity (27 operators), making it less interpretable for practical use. In Fig. 3(b), many of the baseline parameters have $R^2 < 0.5$, which can be attributed to their poor extrapolation performance, particularly for data where $\log R_{\mathrm{c}} > 20$. Additionally, in this GFA task, the R^2 values for varying forms of the formulas do not reach the high values typically observed ($\sim$0.99) in simpler regression tasks. The highest R^2 value reported here is $\sim$0.95, which likely reflects discrepancies and variations across different experimental conditions.

To further validate the effectiveness of our method, we conducted ablation experiments. In-context learning, a method that enhances the reasoning ability of LLMs, has been successfully applied to a variety of symbolic regression problems [19]. In our framework, the memory section functions as in-context learning, leveraging previous search trajectories to guide the optimization of formulas. To isolate the contribution of the memory, we performed a control experiment where the
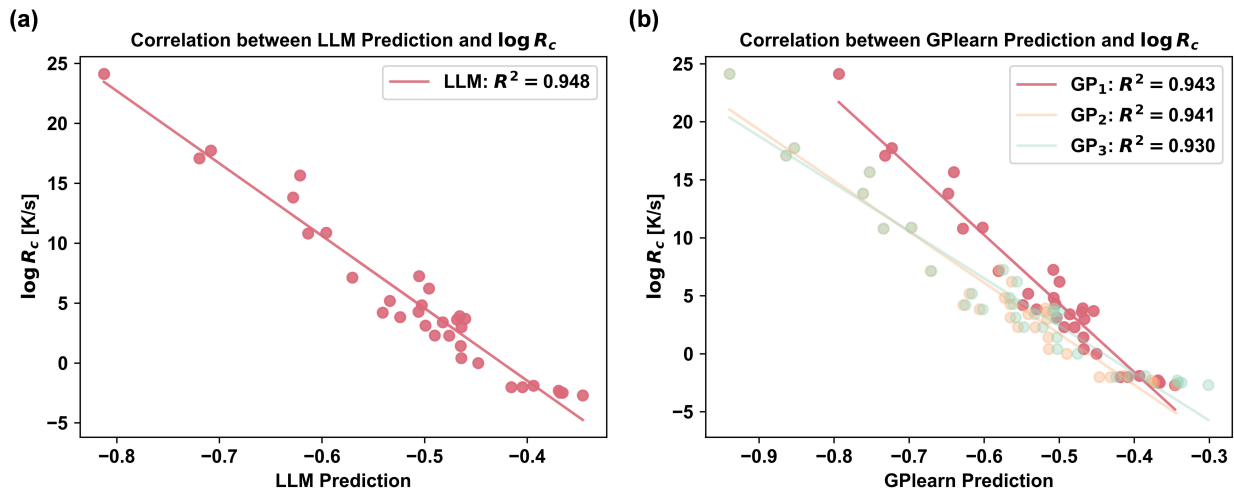
FIG. 2. Comparison of predicted values and experimental critical cooling rate (R_c). (a) Correlation results for the best formula generated by our multi-agent framework. (b) Correlation results of the three best formulas generated by GPlearn [50].
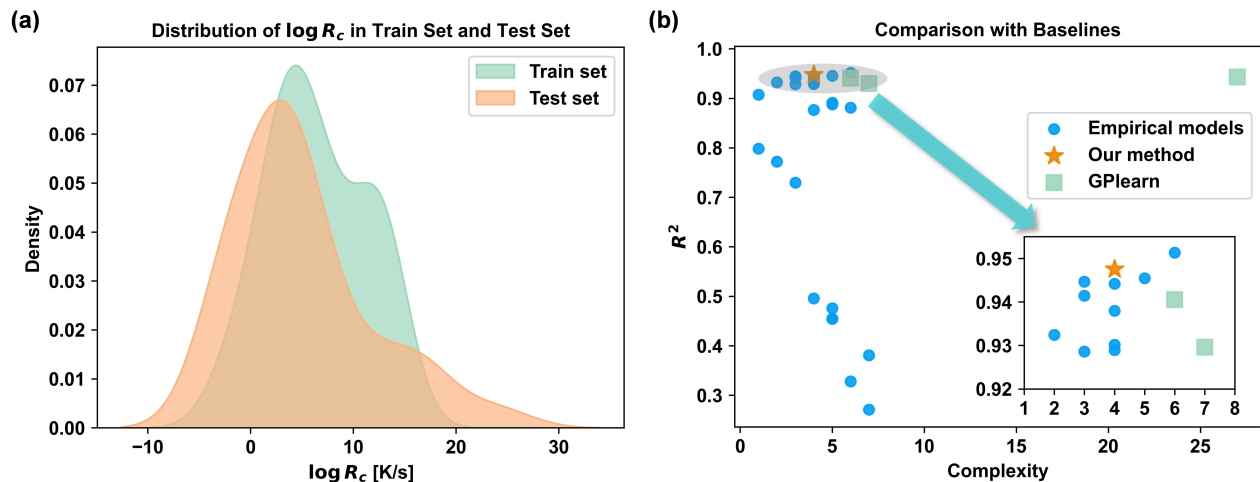

FIG. 3. Data distribution and performance comparison of GFA parameters. (a) Kernel density plot showing the distribution of $\log R_c$ in both the training and test datasets. (b) Comparison of the generated formulas with those obtained using GPlearn and other previously reported GFA parameters.

LLM generated formulas randomly for 5 iterations, without utilizing any prior knowledge. The number of formulas generated is the same as in our framework. As shown in Fig. 4(a), without the influence of prior knowledge, the R^2 value remains low and does not improve much with subsequent iterations for the random guessing method. In contrast, our method, which is guided by prior knowledge, achieves R^2 values greater than 0.90 in each iteration, showing an improvement of ∼30%. This result demonstrates the effectiveness of in-context learning in our task and highlights that LLMs can optimize formula generation without the need for fine-tuning.

In addition to leveraging memory, incorporating self-reflection by LLMs can further enhance their reasoning capabilities. In our workflow, another agent based on LLMs was introduced to reflect on the generated trajectory and provide feedback to the generation agent in Fig. 1(a). Instead of using the same agent for both generation and learning from the trajectory, we utilize a separate reflection agent to give verbal feedback. This approach helps mitigate the "lost in the middle" problem [51], where the performance of LLMs can be influenced by the placement of information in the prompt. By focusing solely on the trajectory, the reflection agent can effectively provide suggestions, ensuring that the information within the trajectory is fully utilized. To evaluate the impact of the reflection component, we compared the performance of the framework with and without the reflection agent. Since the reflection agent influences both the complexity and accuracy of the generated formulas at each step, we compared the average scores and formula complexities of each step across three repeated experiments. As shown in Fig 4(b), without the
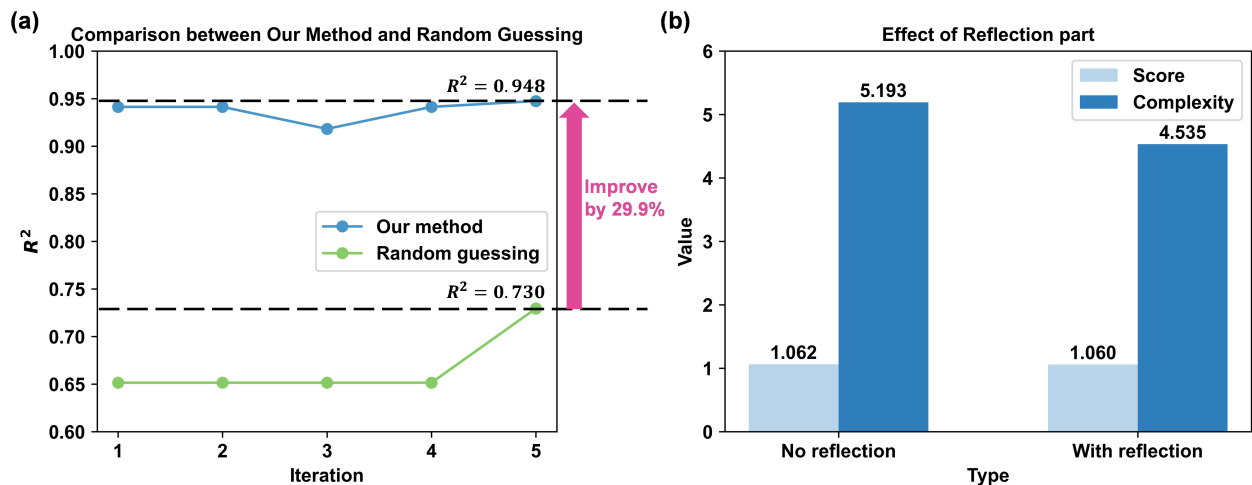
FIG. 4. Impact of memory and self-reflection components on the performance of the framework . (a) Comparison of performance between the proposed method and a random guessing approach without the memory section. (b) Performance comparison with and without the self-reflection component, highlighting its effect on accuracy and formula complexity.
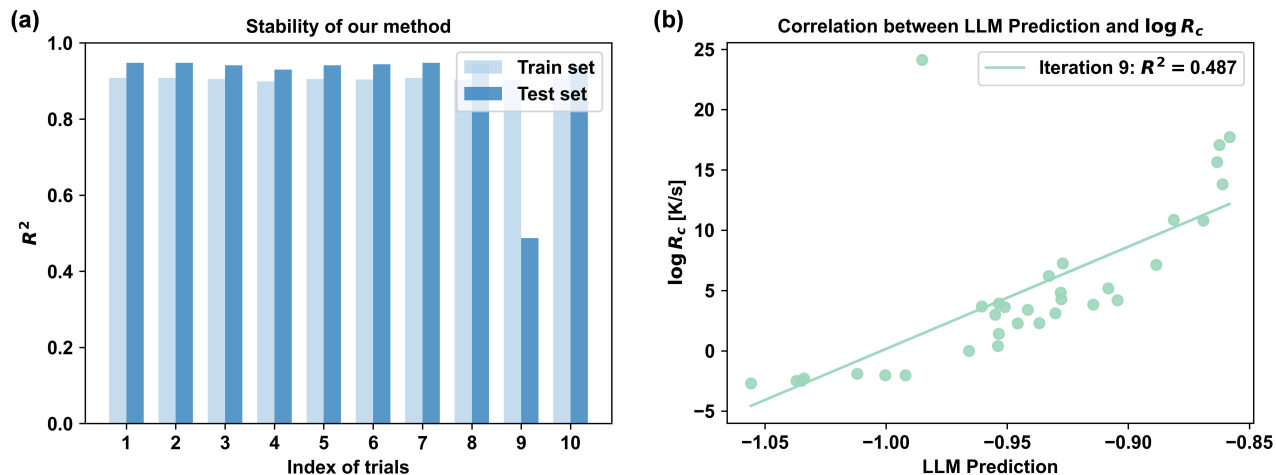

FIG. 5. Stability of the proposed framework. (a) R^2 values from 10 repeated experiments with identical setups, demonstrating consistent performance across trials. (b) Example of a failure in the 9th iteration of the stability test, caused by an "out-of-domain" data point.

reflection agent, the score increases slightly, while the complexity rises significantly from 4.5 to 5.2. This suggests that the reflection agent plays a critical role in controlling formula complexity while improving the overall performance.

By analyzing the suggestions provided by the reflection agent at each step, we can better understand its operational mechanism. The suggestions can be classified into six types. (1) summarizing the trends in the trajectory, (2) identifying terms that frequently appear in high-performing or low-performing formulas (e.g., suggesting the inclusion of terms like (T_g/T_l) in new formulas based on its performance), (3) simplifying complex terms, such as replacing $(T_g/T_l) * (T_l/T_x)$ with (T_g/T_x), (4) proposing new techniques or terms to improve the performance, (5) correcting units errors, and (6) reiterating instructions, such as the need to balance sim-

plicity and performance or to avoid introducing unnormalized constants or terms.

Given the inherent randomness in LLM generation, we incorporate repeated iterations of DFS to enhance the stability of the final results. To further assess the stability of our method, we conducted 10 repeated experiments with identical setups, analyzing the results on both the training and test sets. As shown in Fig. 5(a), all experiments performed well on the training set, with $R^2 > 0.90$. However, one experiment failed on the test set, which was due to a single "out-of-domain" data point, as illustrated in Fig. 5(b). Despite this, 90% of the experiments achieved high R^2 values on the test set, demonstrating the overall stability of our framework.

Discussion

Symbolic regression offers explicit formulas that enhance interpretability, enabling deeper insights into physical phenomena. Fig. 2(a) shows that the GFA predicted by the top derived formula ($F = 0.76(T_g/T_l) - T_g/T_x$) has a negative correlation with experimentally measured $\log R_c$. During the alloy cooling process, a higher critical cooling rate indicates that the material requires rapid cooling to form an amorphous structure, as slower cooling would lead to crystallization. Thus, a larger critical cooling rate corresponds to lower GFA, aligning with the predicted negative correlation.

The formula combines two distinct terms: T_g/T_l, a well-known metric called the reduced glass transition temperature, and T_g/T_x, a newly emphasized parameter, with a balanced coefficient 0.76. The term T_g/T_l first proposed in [26], is positively correlated with GFA. Physically, T_g/T_l represents the ratio between the glass transition temperature (T_g) and the liquidus temperature (T_l). As discussed in [52], a higher T_g/T_l implies a narrower temperature range between T_g and T_l, making it easier for the alloy to bypass crystallization during cooling, thereby enhancing its GFA. This parameter effectively quantifies the ability of a material to form glasses.

In contrast, the second term T_g/T_x shows a negative correlation with GFA. This term can also be expressed as

$$\frac{T_g}{T_x} = -\frac{T_x - T_g}{T_x} + 1 = -\frac{\Delta T_x}{T_x} + 1 \tag{3}$$

where ΔT_x is a widely used GFA parameter. From the perspective of devitrification [32], a larger ΔT_x indicates a broader temperature window where the supercooled liquid phase exists. While this suggests better resistance to crystallization, it also highlights increased competition between crystalline and amorphous phase formation. Therefore, a smaller dimensionless ratio T_g/T_x is associated with higher GFA. The combination of $0.76(T_g/T_l)$ and $-T_g/T_x$ of our method reflects both the ability to form glasses and the resistance to crystallization, achieving a high R^2 with $\log R_c$. This demonstrates the formula robustness and capability to capture the dual factors influencing GFA in metallic glasses.

We present a multi-agent framework designed to address symbolic regression tasks and discover materials laws. To demonstrate the effectiveness of this framework, we apply it to a material science problem focused on GFA. This framework leverages the concept of in-context learning by incorporating the search trajectory from DFS into the optimization loop, thereby enhancing the reasoning ability of LLMs. Specifically, we mainly employ two LLM-based agents: one for formula generation and the other for reflection, with the latter improving the framework through a feedback mechanism.

Our framework provides a general workflow for solving symbolic regression tasks using LLMs, capitalizing on pretrained knowledge and the reflection mechanism. Unlike black-box AI models, the theoretical laws generated by our framework are interpretable and possess low complexity. This approach is extendable to other symbolic regression tasks and can be applied to materials laws discovery in diverse domains.

In the case of GFA, we derived a new formula with low complexity and high accuracy ($R^2 = 0.948$). With appropriate modifications to the dataset and task description, our method can be adapted to solve other symbolic regression problems in physical sciences. The results from this framework can contribute to various downstream applications, such as materials design, interpretation of materials properties, and the identification of descriptors for further machine learning tasks.

However, some limitations remain. The frequent interactions with the LLMs API are time-consuming, which slows down both the search process and the overall computational efficiency. Additionally, our current framework executes a full DFS, meaning that it searches through all nodes in the tree (Fig. 1), which can be also computationally expensive. Therefore, future improvements should focus on simplifying and accelerating the equation search process.

Looking ahead, there are several opportunities to enhance the efficiency of the framework. Currently, our framework handles numerical data, but much of the data in materials science is presented in mixed formats, including textual, numerical, tabular, and visual forms (e.g., SEM images, XRD patterns). Developing a multimodal LLM-based framework could allow us to process these diverse data types more effectively. Furthermore, physical laws–such as the law of universal gravitation–are inherently complex and require large search spaces. To address this challenge, reducing the search space will be critical. Incorporating physical properties like dimensional constraints and symmetries can help simplify the problem and narrow the search space, leading to more efficient solutions.

Methods

Depth-first search Algorithm

The optimization of formulas is mainly achieved through depth-first search (DFS) algorithms. The DFS appraoch for formula optimization is inspired by the Tree-of-Thought (ToT) prompt strategy [53], which utilizes a tree structure to aid language models for reasoning, using either depth-first search or breadth-first search. In symbolic regression tasks, the goal is to optimize formulas to achieve high accuracy. DFS incorporates recursion and backtracking to explore and refine potential solutions. The pseudo-code for this algorithm is presented in Algorithm 1.

Algorithm 1 Depth-first search

1: **Function:** DFS
2: **Input Parameters:** depth d, trajectory T, data Db
3: **if** $d == 0$ **then**
4:     Set initial formulas list f = invoke_generation ()
5: **else**
6:     Set reflection Re = invoke_reflection (T)
7:     Set new formulas list f = invoke_generation (T, Re)
8: **end if**
9: Delete wrong formulas fc = check_formulas (f, Db)
10: **for** F in fc **do**
11:     Set $score\_F$ = evaluate (F, Db)
12:     Update $best\_function, best\_score$
13:     DFS $(d + 1, T + \{F, score\_F\}, Db)$
14: **end for**

LLM setup and Prompt

In this work, *deepseek-chat* [54] was used as the base LLM, which is an open-source LLM specialized in coding tasks. The Python library *langchain* [55], a framework for building applications based on LLMs, was utilized to construct the agents, integrate model interfaces, set up prompt templates, and create task chains. We developed three LLM-based agents for generation, translation and reflection tasks. The generation agent is responsible for generating new formulas based on the task description, previous memory and suggestions from the reflection agent. The translation agent converts the generated formulas, expressed in mathematical notions, into executable Python code for further evaluation and analysis. The reflection agent offers optimization suggestions by reflecting on the previous trajectorys. The structure of the prompt template used to guide the agents is present in Supplementary Figs. **??**, **??** and **??**, respectively. These templates can be customized by adjusting the task descriptions, allowing the framework to be extended for various symbolic regression tasks. In this work, we employ "few-shot" learning approach, where only a few learning examples are provided to the LLMs to guide them in generating results in the desired formats. Using these templates, the agents can be easily constructed based on the *deepseek-chat* [54] language model.

Data availability

The 56 metallic glasses, along with their corresponding characteristic temperatures and critical cooling rates, are listed in Supplementary Information.

Code availability

All the codes used in the paper will be made publicly available on GitHub upon acceptance of the manuscript, and can be provided upon reasonable requests.

References

[1] S.-M. Udrescu and M. Tegmark, AI Feynman: A physics-inspired method for symbolic regression, Science Advances **6**, eaay2631 (2020).

[2] A. White, The Materials Genome Initiative: One year on, MRS Bulletin **37**, 715 (2012).

[3] A. Jain, S. P. Ong, G. Hautier, W. Chen, W. D. Richards, S. Dacek, S. Cholia, D. Gunter, D. Skinner, G. Ceder, and K. A. Persson, Commentary: The Materials Project: A materials genome approach to accelerating materials innovation, APL Materials **1**, 011002 (2013).

[4] S. Curtarolo, W. Setyawan, G. L. W. Hart, M. Jahnatek, R. V. Chepulskii, R. H. Taylor, S. Wang, J. Xue, K. Yang, O. Levy, M. J. Mehl, H. T. Stokes, D. O. Demchenko, and D. Morgan, AFLOW: An automatic framework for high-throughput materials discovery, Computational Materials Science **58**, 218 (2012).

[5] E. Gossett, C. Toher, C. Oses, O. Isayev, F. Legrain, F. Rose, E. Zurek, J. Carrete, N. Mingo, A. Tropsha, and S. Curtarolo, AFLOW-ML: A RESTful API for machine-learning predictions of materials properties, Computational Materials Science **152**, 134 (2018).

[6] D. Zagorac, H. Müller, S. Ruehl, J. Zagorac, and S. Rehme, Recent developments in the Inorganic Crystal Structure Database: Theoretical crystal structure data and related features, Journal of Applied Crystallography **52**, 918 (2019).

[7] X. Yang, Z. Wang, X. Zhao, J. Song, M. Zhang, and H. Liu, MatCloud: A high-throughput computational infrastructure for integrated management of materials simulation, data and resources, Computational Materials Science **146**, 319 (2018).

[8] G. Wang, E. Wang, Z. Li, J. Zhou, and Z. Sun, Exploring the mathematic equations behind the materials science data using interpretable symbolic regression, Interdisciplinary Materials **3**, 637 (2024).

[9] Q. Tao, P. Xu, M. Li, and W. Lu, Machine learning for perovskite materials design and discovery, npj Computational Materials **7**, 1 (2021).

[10] D. Jha, L. Ward, A. Paul, W.-k. Liao, A. Choudhary, C. Wolverton, and A. Agrawal, ElemNet: Deep Learning the Chemistry of Materials From Only Elemental Composition, Scientific Reports **8**, 17593 (2018).

[11] H. Wang, T. Fu, Y. Du, W. Gao, K. Huang, Z. Liu, P. Chandak, S. Liu, P. Van Katwyk, A. Deac, A. Anandkumar, K. Bergen, C. P. Gomes, S. Ho, P. Kohli, J. Lasenby, J. Leskovec, T.-Y. Liu, A. Manrai, D. Marks, B. Ramsundar, L. Song, J. Sun, J. Tang, P. Veličković, M. Welling, L. Zhang, C. W. Coley, Y. Bengio, and M. Zitnik, Scientific discovery in the age of artificial intelligence, Nature **620**, 47 (2023).

[12] D. Angelis, F. Sofos, and T. E. Karakasidis, Artificial Intelligence in Physical Sciences: Symbolic Regression Trends and Perspectives, Archives of Computational Methods in Engineering **30**, 3845 (2023).

[13] J. R. Koza, Genetic programming as a means for programming computers by natural selection, Statistics and Computing **4**, 87 (1994).

[14] M. Landajuela, C. S. Lee, J. Yang, R. Glatt, C. P. Santiago, I. Aravena, T. Mundhenk, G. Mulcahy, and B. K. Petersen, A unified framework for deep symbolic regression, in *Advances in Neural Information Processing Systems*, Vol. 35, edited by S. Koyejo, S. Mohamed, A. Agarwal, D. Belgrave, K. Cho, and A. Oh (Curran Associates, Inc., 2022) pp. 33985–33998.

[15] B. K. Petersen, M. Landajuela, T. N. Mundhenk, C. P. Santiago, S. K. Kim, and J. T. Kim, Deep symbolic regression: Recover-

ing mathematical expressions from data via risk-seeking policy gradients (2021), arXiv:1912.04871.

[16] P. Shojaee, K. Meidani, A. Barati Farimani, and C. Reddy, Transformer-based planning for symbolic regression, in *Advances in Neural Information Processing Systems*, Vol. 36, edited by A. Oh, T. Naumann, A. Globerson, K. Saenko, M. Hardt, and S. Levine (Curran Associates, Inc., 2023) pp. 45907–45919.

[17] M. Cranmer, A. Sanchez-Gonzalez, P. Battaglia, R. Xu, K. Cranmer, D. Spergel, and S. Ho, Discovering Symbolic Models from Deep Learning with Inductive Biases (2020), arXiv:2006.11287.

[18] B. Weng, Z. Song, R. Zhu, Q. Yan, Q. Sun, C. G. Grice, Y. Yan, and W.-J. Yin, Simple descriptor derived from symbolic regression accelerating the discovery of new perovskite catalysts, Nature Communications 11, 3513 (2020).

[19] M. Merler, K. Haitsiukevich, N. Dainese, and P. Marttinen, In-context symbolic regression: Leveraging large language models for function discovery, in *Proceedings of the 62nd Annual Meeting of the Association for Computational Linguistics (Volume 4: Student Research Workshop)*, edited by X. Fu and E. Fleisig (Association for Computational Linguistics, Bangkok, Thailand, 2024) pp. 427–444.

[20] P. Shojaee, K. Meidani, S. Gupta, A. B. Farimani, and C. K. Reddy, LLM-SR: Scientific Equation Discovery via Programming with Large Language Models (2024), arXiv:2404.18400.

[21] M. Du, Y. Chen, Z. Wang, L. Nie, and D. Zhang, LLM4ED: Large Language Models for Automatic Equation Discovery (2024), arXiv:2405.07761.

[22] Q. Wu, G. Bansal, J. Zhang, Y. Wu, B. Li, E. Zhu, L. Jiang, X. Zhang, S. Zhang, J. Liu, A. H. Awadallah, R. W. White, D. Burger, and C. Wang, AutoGen: Enabling Next-Gen LLM Applications via Multi-Agent Conversation (2023), arXiv:2308.08155.

[23] G. Li, H. Hammoud, H. Itani, D. Khizbullin, and B. Ghanem, Camel: Communicative agents for "mind" exploration of large language model society, in *Advances in Neural Information Processing Systems*, Vol. 36, edited by A. Oh, T. Naumann, A. Globerson, K. Saenko, M. Hardt, and S. Levine (Curran Associates, Inc., 2023) pp. 51991–52008.

[24] N. Shinn, F. Cassano, A. Gopinath, K. Narasimhan, and S. Yao, Reflexion: language agents with verbal reinforcement learning, in *Advances in Neural Information Processing Systems*, Vol. 36, edited by A. Oh, T. Naumann, A. Globerson, K. Saenko, M. Hardt, and S. Levine (Curran Associates, Inc., 2023) pp. 8634–8652.

[25] Z. Gou, Z. Shao, Y. Gong, Y. Shen, Y. Yang, N. Duan, and W. Chen, CRITIC: Large Language Models Can Self-Correct with Tool-Interactive Critiquing (2024), arXiv:2305.11738.

[26] D. Turnbull, Under what conditions can a glass be formed?, Contemporary Physics 10, 473 (1969).

[27] X. Li, S. Kou, C. Li, Y. Zhao, and Y. Ding, A criterion of glass-forming ability and stability derived from pseudo-four characteristic temperatures, Intermetallics 134, 107201 (2021).

[28] R. Deng, Z. Long, L. Peng, D. Kuang, and B. Ren, A new mathematical expression for the relation between characteristic temperature and glass-forming ability of metallic glasses, Journal of Non-Crystalline Solids 533, 119829 (2020).

[29] C. Yang, X. Wang, Y. Lu, H. Liu, Q. V. Le, D. Zhou, and X. Chen, Large language models as optimizers, in *The Twelfth International Conference on Learning Representations* (2024).

[30] Y. A. Yadkori, I. Kuzborskij, A. György, and C. Szepesvári, To Believe or Not to Believe Your LLM (2024), arXiv:2406.02543.

[31] M.-X. Li, Y.-T. Sun, C. Wang, L.-W. Hu, S. Sohn, J. Schroers, W.-H. Wang, and Y.-H. Liu, Data-driven discovery of a universal indicator for metallic glass forming ability, Nature Materials 21, 165 (2022).

[32] Z. P. Lu and C. T. Liu, A new glass-forming ability criterion for bulk metallic glasses, Acta Materialia 50, 3501 (2002).

[33] J. Xiong and T.-Y. Zhang, Data-driven glass-forming ability criterion for bulk amorphous metals with data augmentation, Journal of Materials Science & Technology 121, 99 (2022).

[34] A. Inoue, T. Zhang, and T. Masumoto, Glass-forming ability of alloys, Journal of Non-Crystalline Solids 156–158, 473 (1993).

[35] X. Xiao, F. Shoushi, W. Guoming, H. Qin, and D. Yuanda, Influence of beryllium on thermal stability and glass-forming ability of Zr–Al–Ni–Cu bulk amorphous alloys, Journal of Alloys and Compounds 376, 145 (2004).

[36] K. Mondal and B. S. Murty, On the parameters to assess the glass forming ability of liquids, Journal of Non-Crystalline Solids 351, 1366 (2005).

[37] Q. Chen, J. Shen, D. Zhang, H. Fan, J. Sun, and D. McCartney, A new criterion for evaluating the glass-forming ability of bulk metallic glasses, Materials Science and Engineering: A 433, 155 (2006).

[38] X. H. Du, J. C. Huang, C. T. Liu, and Z. P. Lu, New criterion of glass forming ability for bulk metallic glasses, Journal of Applied Physics 101, 086108 (2007).

[39] G. J. Fan, H. Choo, and P. K. Liaw, A new criterion for the glass-forming ability of liquids, Journal of Non-Crystalline Solids 353, 102 (2007).

[40] X. H. Du and J. C. Huang, New criterion in predicting glass forming ability of various glass-forming systems, Chinese Physics B 17, 249 (2008).

[41] Z.-Z. Yuan, S.-L. Bao, Y. Lu, D.-P. Zhang, and L. Yao, A new criterion for evaluating the glass-forming ability of bulk glass forming alloys, Journal of Alloys and Compounds 459, 251 (2008).

[42] Z. Long, H. Wei, Y. Ding, P. Zhang, G. Xie, and A. Inoue, A new criterion for predicting the glass-forming ability of bulk metallic glasses, Journal of Alloys and Compounds 475, 207 (2009).

[43] X.-l. Ji and Y. Pan, A thermodynamic approach to assess glass-forming ability of bulk metallic glasses, Transactions of Nonferrous Metals Society of China 19, 1271 (2009).

[44] G.-H. Zhang and K.-C. Chou, A criterion for evaluating glass-forming ability of alloys, Journal of Applied Physics 106, 094902 (2009).

[45] S. Guo and C. T. Liu, New glass forming ability criterion derived from cooling consideration, Intermetallics 18, 2065 (2010).

[46] M. K. Tripathi, S. Ganguly, P. Dey, and P. P. Chattopadhyay, Evolution of glass forming ability indicator by genetic programming, Computational Materials Science 118, 56 (2016).

[47] Z. Long, W. Liu, M. Zhong, Y. Zhang, M. Zhao, G. Liao, and Z. Chen, A new correlation between the characteristics temperature and glass-forming ability for bulk metallic glasses, Journal of Thermal Analysis and Calorimetry 132, 1645 (2018).

[48] J. Xiong, T.-Y. Zhang, and S.-Q. Shi, Machine learning prediction of elastic properties and glass-forming ability of bulk metallic glasses, MRS Communications 9, 576 (2019).

[49] B. Ren, Z. Long, and R. Deng, A new criterion for predicting the glass-forming ability of alloys based on machine learning, Computational Materials Science 189, 110259 (2021).

[50] T. Stephens, Gplearn, https://github.com/trevorstephens/gplearn (2024).

[51] N. F. Liu, K. Lin, J. Hewitt, A. Paranjape, M. Bevilacqua, F. Petroni, and P. Liang, Lost in the Middle: How Language Models Use Long Contexts (2023), arXiv:2307.03172.

[52] Z. P. Lu, Y. Li, and S. C. Ng, Reduced glass transition temperature and glass forming ability of bulk glass forming alloys, Journal of Non-Crystalline Solids **270**, 103 (2000).

[53] S. Yao, D. Yu, J. Zhao, I. Shafran, T. Griffiths, Y. Cao, and K. Narasimhan, Tree of thoughts: Deliberate problem solving with large language models, in *Advances in Neural Information Processing Systems*, Vol. 36, edited by A. Oh, T. Naumann, A. Globerson, K. Saenko, M. Hardt, and S. Levine (Curran Associates, Inc., 2023) pp. 11809–11822.

[54] DeepSeek-AI, DeepSeek-V2: A Strong, Economical, and Efficient Mixture-of-Experts Language Model (2024), arXiv:2405.04434.

[55] langchain ai, Langchain, https://github.com/langchain-ai/langchain (2024).

[56] T. Wen, W. Yao, and N. Wang, Correlation between the Arrhenius crossover and the glass forming ability in metallic glasses, Scientific Reports **7**, 13164 (2017).

Competing interests

The authors declare no competing interests.